J. REDUTKO©1*, A. KALWIK©1, A. SZAREK©1

CHANGES IN THERMAL PROPERTIES OF PRINTOUTS MADE OF PETG AND PLA DOPED WITH COPPER AFTER ELECTROCORROSIVE AGEING PROCESS

The article presents the results of research on selected thermal, mechanical properties, as well as the microscopic structure of filaments and details made on a 3D printer in FDM technology. The materials used in the study were PETG (polyethylene terephthalate doped with glycol) and PLA (polylactide) doped with copper. As part of the study, Differential Scanning Calorimetry (DSC) was performed in order to determine the temperatures of phase transformations and changes in melting enthalpy values of filaments before the printing process and also elements made of them. The second part of the research was electrocorrosive ageing process of printouts, carried out in the Simulated Body Fluid solution in a device generating 0.3 A direct current, voltage with value 4.3 V for the entire duration of the test, which was 720 h. After this process DSC test was conducted again. The next stage of the research was Dynamic Mechanical Analysis (DMA) of printouts before and after electrocorrosive ageing process. This test was carried out to characterize the dynamic-mechanical properties as a function of frequency, temperature and time. Additionally, microscopic analyses of the surfaces of the tested printouts were performed in order to assess the changes after electrolysis.

Keywords: 3D printing; thermal properties; DMA; DSC;Simulated Body Fluid conditions

1. Introduction

3D printing has become extremely popular in the last two decades. Not only because of the short time to make a prototype part, but also because of the increasingly better mechanical strength and surface quality of the printouts. The time of the 2019-nCoV coronavirus pandemic has led to significant development of this technology. Many of the components used to modify medical devices, personal protective equipment, and diagnostic support components were manufactured using 3D printing technology at the time. Regardless of the technology applied to create the printouts, their high quality and durability as well as biocompatibility of the materials that they are made of, have recently turned out to be extremely important [1-4].

3D printers in FDM (Fused Deposition Modeling), SLA (Sterolitography) and DLP (Digital Light Processing) technologies have recently become a part of equipment of many hospitals and dental surgeries. This is because of its ability to quickly and reliably replicate models developed from patient diagnostic imaging studies, and also as an enabler and modifier of existing medical devices with which today's hospitals are filled. Additionally, the possibility of using printouts in the patient's body is becoming more common [5-9]. The scale, with which 3D printers are arriving, shows how modern rapid prototyping methods are needed for the development of medicine [7-12].

Printouts for medical applications, incl. surgical instruments, bone screw guides, and implants, should be thoroughly tested in terms of biocompatibility, mechanical strength and thermal resistance. Elements for medical purposes made with this technology should be characterized by considerable resistance to procedures related to their sterilization at elevated temperature and pressure, as well as to chemicals used during disinfection [6,7,13].

The aim of the presented research was to evaluate the effect of electrochemical ageing in the Simulated Body Fluid on the thermal properties of printouts made of PLA filaments with an admixture of copper and PETG for medical applications. Attention was also paid to changes during dynamic mechanical analysis and the changes in structure before and after the electocorossion process were assessed during observation with a microscope at a magnification of 200×.

1 CZESTOCHOWA UNIVERSITY OF TECHNOLOGY, FACULTY OF MECHANICAL ENGINEERING AND COMPUTER SCIENCE, DEPARTMENT OF TECHNOLOGY AND AUTOMATION, 21 ARMII KRAJOWEJ AV., 42-201 CZESTOCHOWA, POLAND

* Corresponding author: jredutko@iop.pcz.pl

2. Methods and methodology

The tests were carried out on samples made on a 3D printer in the FDM technology from two types of filaments: PLA with a 3% addition of copper and PETG intended for contact with tissues. Immediately after the printing process, samples were prepared for testing by removing the support material. Then, a preliminary microscopic analysis of the printout surfaces was performed. The next stage of the study was to determine the loss angle tangent and the storage modulus during Dynamic Mechanical Analysis (DMA). Measurements of the thermal effects accompanying the phenomena occurring in the samples were also performed during the differential scanning calorimetry (DSC) test. The next step during the research was to place the samples in a DC generator in the Simulated Body Fluid environment for a period of 720 hours. In the middle of the electrocorrosive test cycle and after its completion, microscopic analyses of the samples were again performed, as well as DSC and DMA tests.

2.1. 3D printer

During the test, a Zortrax M200 Plus 3D printer was used to produce samples with dimensions of 10×56×4 mm with a raft-type support part. Bar models were designed in Autodesk Inventor 2016, then converted to .stl format and divided into layers in Z-Suite ver. 2.16.2.0, in which printing parameters were also selected. Printouts with PLA doped with copper were made with full filling at following parameters: nozzle diameter of 0.4 mm, layer thickness of 0.14 mm, extrusion temperature of 210°C, platform temperature of 30°C. The PETG samples were also printed with full filling at the same nozzle diameter, layer thickness and the platform temperature, but the extrusion temperature for this material was 245°C. For both type of material the speed of printing was determined as 40 mm/s. In presented research the parameters of the process were specified to obtain the best printout resolution.

The samples were printed with a raft, i.e. in the form of a mesh preceding the target print, which was to improve the adhesion of the printout to the working table and eliminate any warping of the first layer. The printed samples were placed on the printer table with the largest surface. How a single sample looked during the printing process is shown in Fig. 1

2.2. Electrocorrosion

The proper part of the research consisted in placing the samples in the shape of beams in a glass container with the Simulated Body Fluid (SBF) solution, the composition of which was as follows: 8.8 g/l NaCl, 0.4 g/l KCl, 0.14 g/l $CaCl_2$, 0.35 g/l $NaHCO_3$, 1.0 g/l $C_6H_6O_6$ (glucose), 0.2 g/l $MgSO_4 \cdot 7H_2O$, 0.1 g/l $KH_2PO_4 \cdot H_2O$, 0.06 g/l $Na_2HPO_4 \cdot 7H_2O$, pH 7.4. The electrolysis process carried out in the SBF solution lasted 720 hours, with direct current of 3.0 A and voltage of 4.3 V supplied to it.
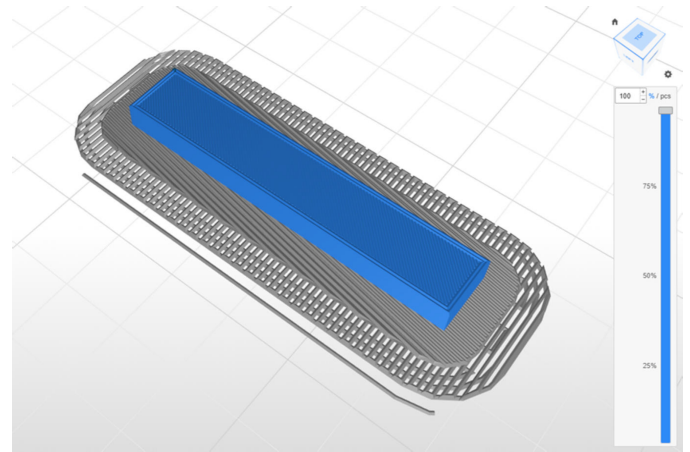

Fig. 1. Preview of the print layout on the printing platform

After completion of the electrochemical ageing process, the samples were thoroughly cleaned with demineralized water in an ultrasonic cleaner, and then tests were performed to determine the thermal properties of the aged printouts [14-17].

2.3. DMA

In the presented research, the dynamic mechanical analysis (DMA) was used to assess changes in the characteristics of thermoplastic samples, which consisted in subjecting the sample to periodically changing mechanical loads (in this case sinusoidal) as a function of temperature. Thanks to it, it is possible to determine the occurrence of anisotropy of mechanical properties of printouts. This study allows determining the dynamic modulus of elasticity E'', the loss modulus E', as well as the tangent of the mechanical loss angle tgσ. When the sample is influenced by the periodically changing vibrations, the strain takes the values determined in [18-21] Eq. (1).

$$\sigma = \sigma_0 \sin \omega t \tag{1}$$

where:
ω – angular frequency; $\omega = 2\pi f = 2\pi/T_0$,
f – frequency,
σ_0 – stress amplitude.

The stresses occurring in the sample are then periodically variable, shifted by the angle $0 < \delta < (\pi/2)$ in relation to the strains Eq. (2):

$$E^* = E' + i \cdot E'' \tag{2}$$

where:
E^* – complex modulus,
E' – the real part of the dynamic modulus,
E' – the imaginary part of the dynamic modulus.

The mechanical loss factor tgδ is the ratio of the modulus of elasticity and the modulus related to the behavior and elastic energy return during deformation [18-21] Eq. (3).

$$\mathrm{tg}\delta = \frac{E''}{E'} \tag{3}$$

The device used during the tests is the NETZSCH DMA 242, which enables testing at any type of dynamic load, depending on the used holder, in the temperature range from –170°C to 600°C. In the presented tests, a grip for three-point free bending of the sample in the form of a beam was used and the following parameters were set: amplitude of 80 μm, frequency of 10 Hz, sample cooling in nitrogen atmosphere, temperature range from –80 to 250°C, samples with dimensions of 10×4×50 mm, sample heating speed 2°C/min. Measurements were made in accordance with ISO 6721:2019 Plastics – Determination of dynamic mechanical properties standard.

2.4. DSC

The method of differential scanning calorimetry (DSC) allows assessing the structure of polymeric materials. This test consists in measuring the thermal effects that accompany the phenomena occurring in the tested samples. The principle of operation of the device is based on the difference in heat flow between the furnace and the tested material, and between the furnace and the reference sample under the influence of a specific temperature [19-23] Eq. (4).

$$\Phi m = \Phi S - \Phi R \qquad (4)$$

where:
  Φm – flow of heat fluxes,
  ΦS – flow of heat tested in measurement with the sample,
  ΦR – flow of heat tested in measurement with the sample with an empty crucible.

The principle of the device working is based on placing the empty crucible and the crucible with a prepared sample on the disk, with some thermocouples, providing heat energy to the space, and then measurement of flow of heat stream. The amount of the entire transmitted heat (Q) was corresponded to the time related with intensity of heat flow [18, 22-24] Eq. (5).

$$Q = \int \frac{dQ}{dt} dt \qquad (5)$$

The amount of heat transferred per unit time (dQ/dt) is defined as the heat flow rate and is expressed in watts (W). In turn, the content of the crystalline phase is determined from the following expression [18] Eq. (6).

$$\alpha_j = \frac{\Delta H_j}{\Delta H_{tot,T}} \times 100\% \qquad (6)$$

where:
  ΔH_j – sample melting enthalpy in J/g determined from the thermogram,
  $\Delta H_{tot,T}$ – theoretical enthalpy of fusion for a fully crystalline polymer.

The test performed on the 214 Polyma NETZSCH DSC device made it possible to determine the degree of crystallinity, melting and crystallization temperature, as well as the glass transition temperature of the test printouts. The research material was taken from the top layer of the printouts due to the contact with the electrocorrosive environment. Measurements were made in accordance with PN-EN ISO 11357-1:2016-11 standard [23], with a heating speed of 10 K/min. The obtained results were developed in the Proteus Analysis program.

3. Results and discussion

As part of the presented work, a comparative analysis of the DSC thermograms of the printed samples before the electrocorrosion process (the first tested sample), after 2 weeks (the second tested sample) and after 4 weeks in corrosive conditions (the third tested sample) was performed. The curves obtained during this test are shown in Figs. 1-4. The analysis of the first heating curves of PETG printouts showed slight changes in the glass transition temperature of the samples. In the printout before the electro-ageing process, the value of this temperature was 79.1°C, after 360 h of electrocorrosion, the temperature increased to 79.6°C,
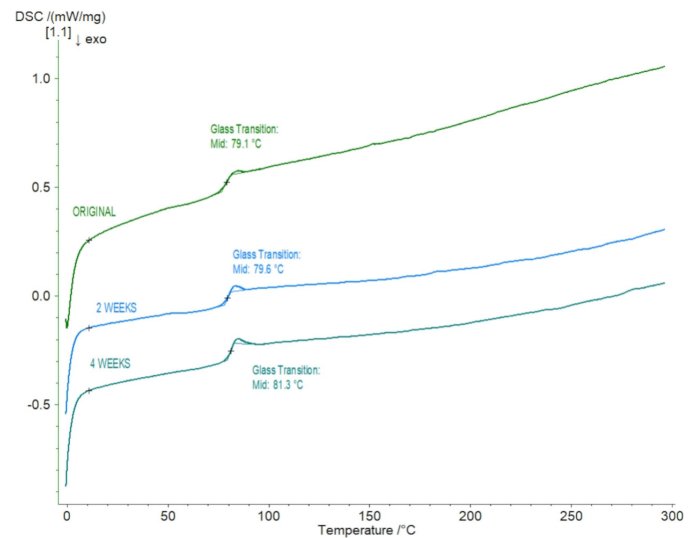

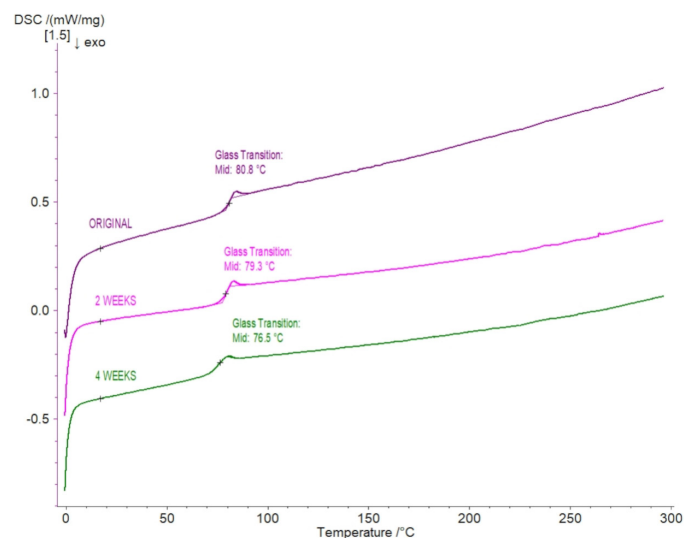Fig. 2. DSC thermograms of PETG printouts first heating

Fig. 3. DSC thermograms of PETG printouts second heating

while after the end of the test cycle, its value was 81.3°C. During the second heating to remove the thermal history of the samples, the glass transition temperature dropped significantly: for the original sample it was 80.8°C, for the sample after two weeks it was 79.3°C, and after 4 weeks it was 76.5°C.

On the DSC thermograms of PLA with a 3% addition of copper, the glass transition temperature during the first heating was respectively 64.6°C for the original sample, 62.7°C for the sample in the middle of the test cycle and 62.1°C for the sample subjected to electrocorrosion the longest. Additionally, on the sample not placed in the SEM solution, two peaks were observed at the temperature of 150.5°C and 155.4°C, while the melting enthalpy was 49.56 J/g. After the first heating of the samples after half and after the entire electrocorrosion cycle, peaks are observed at a very similar temperature of 159.8°C and 159.6°C, however, the change occurred in the melting enthalpy, which for the sample subjected to electrocorrosion was 58.48 J/g, for the next sample was 56.6 J/g. The glass transition temperature of the samples after the second heating was: 61.5°C for the sample
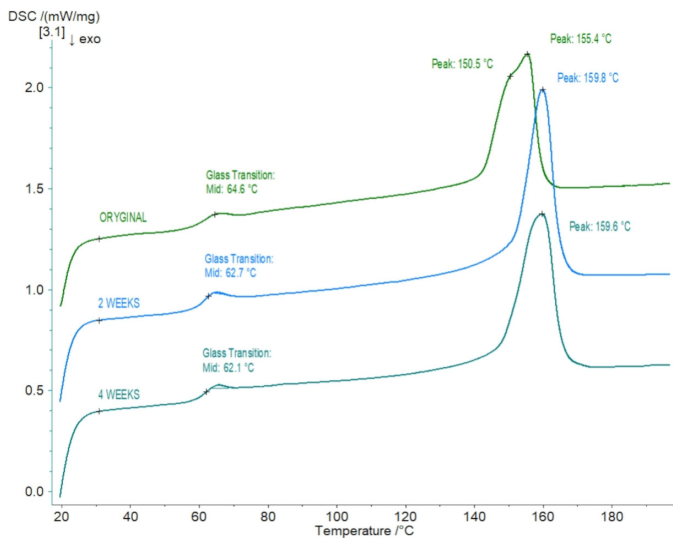
not subjected to electrocorrosion, 61.1°C after 360 h and 60.8°C after 720 h. These thermograms also show peaks with a value of 101.1°C with a melting enthalpy of -8.06 J/g, and a peak of 150.5°C with a melting enthalpy of 47.2 J/g and a peak value of 154.9°C for the original sample. During the second heating of the sample after two weeks in an electrocorrosive environment, the peaks had a value of 102.4°C with a melting enthalpy of –12.1 J/g, another one with a value of 150.6°C and another with a value of 155°C and a melting enthalpy of 43.12 J/g. The next thermogram of the second sample heating after the entire ageing cycle shows the first peak of 130°C with a melting enthalpy of –13.1 J/g and the second one of 154.7°C, the melting enthalpy in this case was 14.7 J/g.

The next stage of the research was the analysis of the curves obtained during the DMA test. The study consisted in determining the changes in the storage modulus and the tangent of the angle of mechanical losses as a function of the temperature of the samples subjected to electrocorrosion. The analyzed curves are shown in Figs. 5-8.

The storage modulus of PLA printouts with copper admixture at the temperature starting the measurement, i.e. about
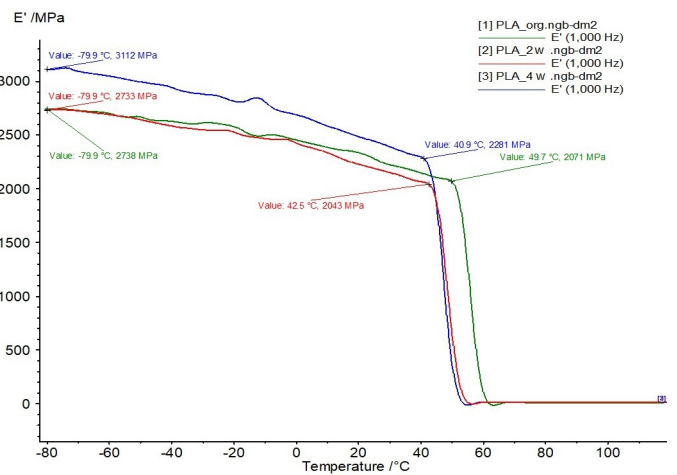

Fig. 4. DSC thermograms of PLA printouts first heating

Fig. 6. Storage module E' dependence on temperature of PLA doped with copper printouts

Fig. 5. DSC thermograms of PLA printouts second heating

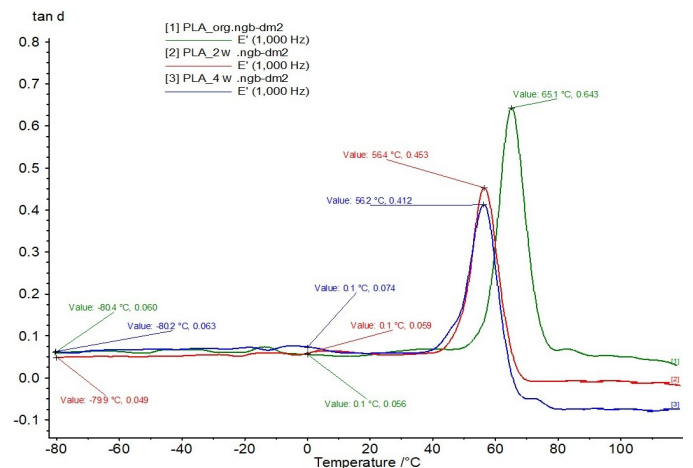
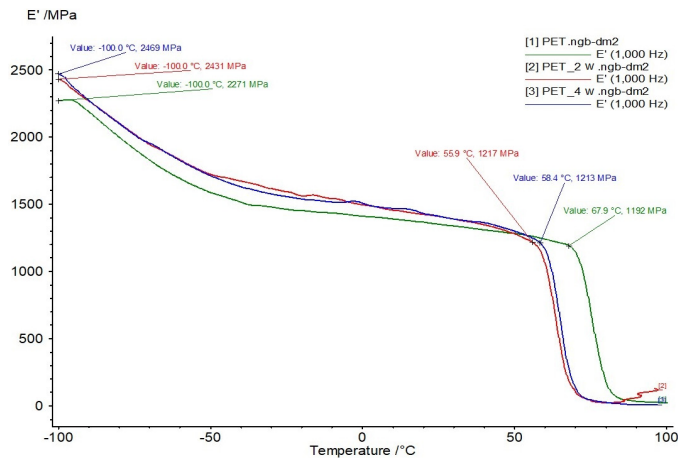Fig. 7. Course of change of tangent values of the mechanical loss angle tgδ for PLA doped with copper printouts tested

Fig. 8. Storage module E' dependence on temperature of PETG printouts

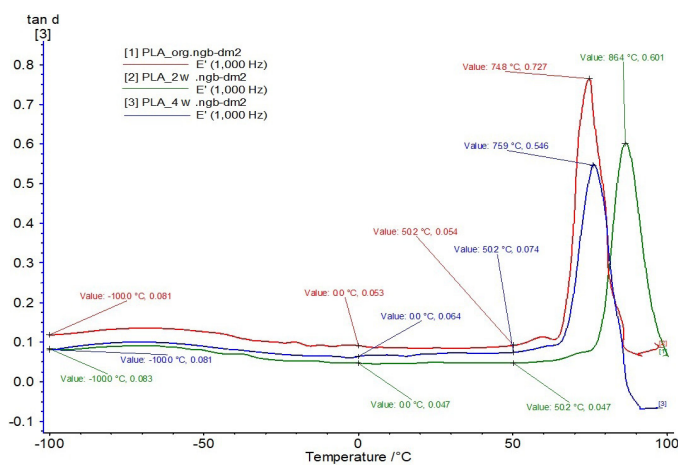Fig. 9. Course of change of tangent values of the mechanical loss angle tgδ for PETG printouts tested

–80°C, was in the range of 2738 MPa for the sample not subjected to electrocorrosion. For the printout tested in the middle of the electrocorrosion cycle, E' was 2733 MPa, while the last polylactide sample tested at this temperature showed the highest storage modulus E' at the level of 3112 MPa. When the temperature in the measuring chamber reached 40.9°C, there was a rapid decrease in the value of the storage modulus of the sample after 4 weeks of electrostatic ageing, starting at the E' value of 2281 MPa. We observe similar decreases at the temperature of 42.5°C

of the sample after two weeks and at the temperature of 49.7°C of the unaged sample.

Analyzing the curves of tangent of the angle of mechanical losses of the PLA printouts as a function of temperature, it can be noticed that at –80°C and 0°C the tgδ values were very similar, as they ranged from 0.056 to 0.074. The value of the analyzed parameter increased at the temperature of about 45°C in the case of samples subjected to electrocorrosion and at the temperature of 50°C by analyzing the sample just after the printing process. The highest recorded tgδ values for individual samples were: 0.643 at the temperature of 65°C for the original sample, 0.453 at the temperature of 56.4°C for the sample after 2 weeks in the electro-ageing chamber and 0.412 at the temperature of 56.2°C for the longest electro-ageing sample.

The storage modulus of PETG printouts for medical applications at the temperature from which the measurement was started, i.e. –100°C, was respectively: 2469 MPa for a printout subjected to electrocorrosion for 4 weeks, 2431 MPa for a printout after 2 weeks of electro-ageing and 2271 MPa for the original printout. As the temperature in the measuring chamber increased, the E' value gradually decreased until the samples reached values ranging from 1192 MPa at 67.9°C (original sample) to 1217 MPa at 55.9°C (sample after two weeks). After reaching this range of values, there was a sudden drop in the storage modulus of all analyzed printouts.

The values of tangent of the mechanical loss angle at –100°C, 0°C and 50°C for all three samples remained at a similar level, i.e. from 0.081 to 0.054 for the original sample, 0.081 to 0.074 for the sample after 4 weeks, and also 0.083 to 0.047 for the sample after two weeks electro-ageing. More rapid increase was recorded around 73°C for the original sample (peak 0.727 at 74.8°C) and in the middle of the electrostatic cycle (peak 0.546 at 75.9°C), for the last sample a similar increase occurred at around 83°C, reaching the maximum value of 0.601 at 86.4°C.

Microscopic analysis carried out on the Keyence VHX-7000 microscope showed significant changes in all samples after electrocorrosion, both with PLA with the addition of copper and with PETG samples. The microscopic photos are presented in Figs. 9 and 10. The colour of the tested printouts has changed significantly, and the surface structure has changed slightly, which has become more matt. Additionally, it should be noted that along with the time spent in the electro-ageing chamber, the
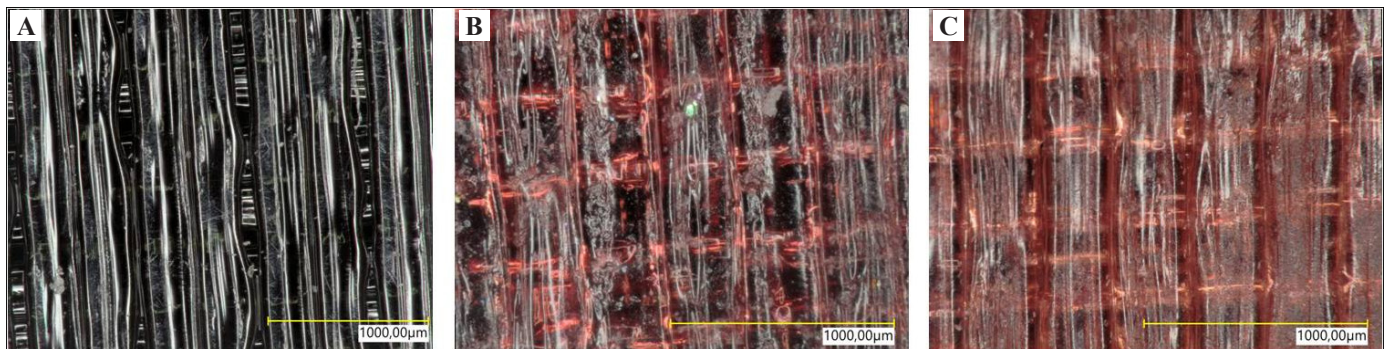

Fig. 10. Microscopic photo of printouts made of PETG at a magnification of 200×: A – original, B – after 2 weeks, C – after 4 weeks
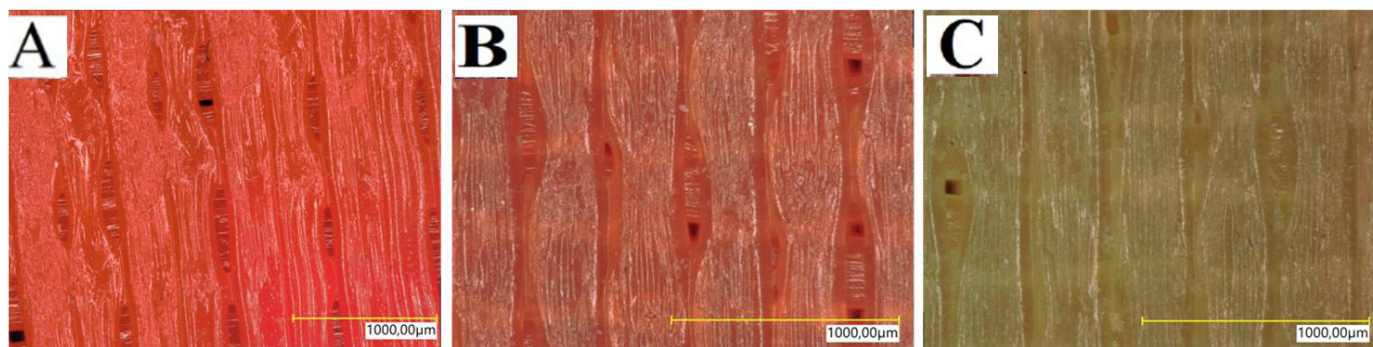
Fig. 11. Microscopic photo of printouts made of PLA doped with copper at a magnification of 200×: A – original, B – after 2 weeks, C – after 4 weeks

PETG samples became more transparent compared to the original printout. Their colour also began to be closer to copper. It should be noted, however, that the tested samples of filament made of PETG and PLA with the addition of copper were not subjected to ageing at the same time. Polylactide samples after two weeks of electrocorrosion in SBF became much darker than the original printouts, after another two weeks their colour completely changed to a green-brown shade. When analysing the spaces between successive threads of the embossed material, it can not be observed any significant changes. The electrocorrosion in the Simulated Body Fluid did not significantly affect the quality of the connection of subsequent layers visible under the microscope.

The conducted research can be classified as innovative research, as there are no publications presenting similar assessments of changes in the mechanical and thermal properties of elements made on 3D printers. It should be noted that the tests performed were aimed at determining the influence of chemically aggressive factors on printouts made of thermoplastic materials admitted contacting with tissues.

It is also necessary to take into account the influence of the structure that characterizes the printouts made with the FDM technology, namely the presence of pores created by the imprecise connection of successive threads of the extruded material. During the electrocorrosion process through these pores, SBF got into the deep layers of the printouts. Due to this penetration, the aging process in the analyzed conditions did not affect only the external surfaces of the printouts, as would be the case with elements made with injection technology. Based on the literature dealing with this subject, it can be concluded that the phenomenon of microporosity of printouts is an inherent feature that occurs when printing elements from thermoplastic materials. This is due to the desired printing parameters such as filament diameter, nozzle diameter and layer height [25-29].

3. Conclusion

The presented research and the analysis of the results show that the electrocorrosion process in the Simulated Body Fluid environment influences to some extent the thermal and mechanical properties of printouts made of filaments dedicated to contact with tissues. It should be noted, however, that the samples subjected to electrocorrosion tested with DSC and DMA devices did not significantly change the properties of the printouts, taking into account the results from the second and fourth week of electrocorrosion.

DSC analysis of the second heat, after eliminating the thermal history of the samples, showed that the melting enthalpy of PLA samples with copper is related to the ageing time in a specific environment. The highest melting enthalpy was recorded for the printout not subjected to ageing, while the lowest for the printout subjected to electrocorrosion the longest. Additionally, these samples show the phenomenon of cold crystallization, which was observed in the sample after four weeks at a temperature higher by about 30°C than in the previous samples. In turn, during the DSC analysis of the second heating of the PETG filament samples, it can also be noticed that the glass transition temperature drops with the time the sample remains in the electrostatic environment.

DMA test of samples from both polylactide and PETG allowed to conclude that with the increase in the staying time of the printouts in the electrocorrosive environment, the value of the tangent of the mechanical loss angle decreases. On the other hand, the analysis of the storage modulus showed that for both tested materials, the E' value of aged samples dropped sharply at temperatures lower than for the original printouts.

Additionally, microscopic analysis allowed concluding that the pigment content in PETG printouts changed during electrocorrosion. However, further detailed studies are needed to determine the phenomena occurring in the tested printouts during electrocorrosion in the SBF environment. When analyzing the presented tests at a later stage, it is necessary to precisely determine the influence of the porous structure visible in the microscopic photos of the printed elements on their thermal and mechanical properties.

Another component that may affect the properties analyzed in the work is the type of the applied model filling pattern. It has been proven that various types of cellular structures that are used as the filling of the element have an impact on energy absorption during durability tests of printouts.

The presented research can be described as preliminary test. The next stage of this research will be to determine the impact of print parameters on thermal and mechanical properties and also, if these parameters are affected by the porosity of printouts.

REFERENCES

[1] S. Ishack, S. Lipner, Am. J. Med. **133** (7), 771-773 (2020).
DOI: https://doi.org/10.1016/j.amjmed.2020.04.002

[2] R. Tino, R. Moore, S. Antoline, P. Ravi, N. Wake, C. Ionita, J. Morris, S. Decker, A. Sheikh, F. Rybicki, 3D Print Med **6**, 11 (2020). DOI: https://doi.org/10.1186/s41205-020-00064-7

[3] D. Amin, N. Nguyen, S. Roser, S. Abramowicz, J. Oral Maxillofac. Surg. **78** (8), 1275-1278 (2020).
DOI: https://doi.org/10.1016/j.joms.2020.04.040

[4] M. Attaran, Am. **J**. Ind. Manag. Optim. **10** (5), 988-1001 (2020).
DOI: https://doi.org/10.4236/ajibm.2020.105066

[5] D. Javaid, P. Haleem, D. Singh, D. Suman, Sustainable Oper. Comput. (2021). DOI: https://doi.org/10.1016/j.susoc.2021.05.002

[6] N. Shahrubudin, P. Koshy, J. Alipal, M. Kadir, T. Lee, Heliyon **6** (4), p.e03734 (2020).
DOI: https://doi.org/10.1016/j.heliyon.2020.e03734

[7] G. Qiu, W. Ding, W. Tian, L. Qin, Y. Zhao, L. Zhang, J. Lu, et. al., Engineering **6** (11), 1217-1221 (2020).
DOI: https://doi.org/10.1016/j.eng.2020.10.002

[8] D. Popescu, F. Baciu, D. Vlăsceanu, C. Cotruţ, R. Marinescu, Mech. Mater. **148**, 103423 (2020).
DOI: https://doi.org/10.1016/j.mechmat.2020.103423

[9] S. Kurenov, C. Ionita, D. Sammons, T. Demmy, J. Thorac Cardiovasc Surg. **149** (4), 973-979 (2015).
DOI: https://doi.org/10.1016/j.jtcvs.2014.12.059

[10] A. Hazeveld, J.J.R. Huddleston Slater, Y. Red, Am. J. Orthod. Dentofac. **145** (1), 108-115 (2014).
DOI: https://doi.org/10.1016/j.ajodo.2013.05.011.

[11] T. Ngo, A. Kashania, G. Imbalzanoa, K. Nguyena D. Huib, Composites Part B **143**, 172-196 (2018).
DOI: https://doi.org/10.1016/j.compositesb.2018.02.012

[12] V. DeStefano, S. Khan, A. Tabada, Eng. Regener. **1**, 76-87 (2020).
DOI: https://doi.org/10.1016/j.engreg.2020.08.002

[13] C. Culmone, G. Smit, P. Breedveld,. Addit. Manuf. **27**, 461-473 (2019). DOI: https://doi.org/10.1016/j.addma.2019.03.015

[14] Y. Song, D. Shan, R. Chen, F. Zhang, E. Han, Mater. Sci. Eng. C, **29** (3), 1039-1045 (2009).
DOI: https://doi.org/10.1016/j.msec.2008.08.026

[15] I. Gurappa, Mater. Charact. **49** (1), 73-79 (2002).
DOI: https://doi.org/10.1016/S1044-5803(02)003200

[16] G. Song, J. Corros. Sci. Eng. **49** (4), 1696-1701 (2007).
DOI: https://doi.org/10.1016/j.corsci.2007.01.001

[17] A. Szarek, A. Gnatowski, Aktualne Problemy Biomechaniki, 5, 153-158 (2011).

[18] E. Bociąga, T. Jaruga, Materiały Niemetalowe, Wydawnictwo Politechniki Częstochowskiej (2013).

[19] R. Sobczak, Z. Nitkiewicz, J. Koszkul, Composites **2** (3), 78-79 (2002).

[20] M. Szumera, LAB Laboratoria, Aparatura, Badania **17** (6), 28-34 (2012).

[21] M. Szumera, LAB Laboratoria, Aparatura, Badania **18** (1), 24-33 (2013).

[22] M. Labus, Nafta-Gaz **75** (1), 3-9 (2019).
DOI: https://doi.org/10.18668/NG.2019.01.01.

[23] PN-EN ISO 11357-1:2016-11 Plastics – Differential Scanning Calorimetry (DSC) – Part1: General principles

[24] ISO 6721:2019 Plastics – Determination of dynamic mechanical properties.

[24] A. Gnatowski, M. Chyra, Przemysł chemiczny **1** (1), 105-109 (2015). DOI: https://doi.org/10.15199/62.2015.1.16

[25] A. Jakus, N. Geisendorfer, P. Lewis, R. Shah, Acta Biomaterialia **72**, 94-109 (2018).
DOI: https://doi.org/10.1016/j.actbio.2018.03.039

[26] M. Kucewicz, P. Baranowski, J. Małachowski, A. Popławski, P. Płatek, Materials & Design **142**, 177-189 (2018).
DOI: https://doi.org/10.1016/j.matdes.2018.01.028

[27] M. Lesueur, T. Poulet, M. Veveakis, Additive Manufacturing **44**, 102061 (2021).
DOI: https://doi.org/10.1016/j.addma.2021.102061

[28] R. Roy, A. Mukhopadhyay, Materials Today: Proceedings **41**, 856-862 (2021).
DOI: https://doi.org/10.1016/j.matpr.2020.09.235

[29] J. Janiszewski, P. Płatek, P. Dziewit, K. Sarzyńska, Problems of Mechatronics Armament Aviation Safety Engineering **9** (3), 29-52 (2018). DOI: https://doi.org/10.5604/01.3001.0012.2738